EPJ Web of Conferences **140**, 09016 (2017) DOI: 10.1051/epjconf/201714009016
*Powders & Grains 2017*

# Self-Structuring of Granular material under Capillary Bulldozing

*Guillaume* Dumazer[1,⋆], *Bjørnar* Sandnes[2], *Monem* Ayaz[1,3], *Knut Jørgen* Måløy[1], and *Eirik* Flekkøy[1]

[1] *Physics Department, University of Oslo, P. O. Box 1048 Blindern Oslo, Norway*
[2] *College of Engineering, Swansea University, Bay Campus, Swansea SA1 8EN, UK*
[3] *Institut de Physique du Globe de Strasbourg, Université de Strasbourg/EOST, CNRS, 5 rue Descartes, F67084 Strasbourg Cedex, France*

**Abstract.** An experimental observation of the structuring of a granular suspension under the progress of a gas/liquid meniscus in a narrow tube is reported here. The granular material is moved and compactifies as a growing accumulation front. The frictional interaction with the confining walls increases until the pore capillary entry pressure is reached. The gas then penetrates the clogged granular packing and a further accumulation front is formed at the far side of the plug. This cyclic process continues until the gas/liquid interface reaches the tube's outlet, leaving a trail of plugs in the tube. Such 1D pattern formation belongs to a larger family of patterning dynamics observed in 2D Hele-Shaw geometry. The cylindrical geometry considered here provides an ideal case for a theoretical modelling for forced granular matter oscillating between a long frictional phase and a sudden viscous fluidization.

## 1 Introduction

Transport of oil, water and sand in sub-sea pipelines [1], of blood cells suspended in plasma [2, 3] give two extreme examples of the broad range of situations featuring the multiphase transport of granular material in confined geometries. Pneumatic transport offers a well established field for the transport of granular particles immersed in a single phase [4]. Such a two phase system shows a broad range of flow regimes depending on the filling fraction and flow rate. Plug flow, fluidized flow, bubbly flow, turbulent fluidization, cluster flow, annular flow and suspended flow gives the variety of flow regimes in vertical pneumatic conveying [5]. Such observed flow regimes involve the competing effects of viscosity and friction [6–8], respectively destabilizing and stabilizing the granular phase.

The case of dense granular suspension has recently been actively studied as it features complex rheological behaviour such as shear thinning, shear thickening, yield stress and shear banding [9–12]. The frictional interaction and contact time between granular particle and the viscous interaction with the carrying fluid are the two factors determining the behaviour of dense suspensions. The geometrical confinement is then another key factor as it produces extra frictional forces on the granular flow. The frictional interaction with boundaries induces contacts network spanning over a large part of the system.

In multiphase flows, the existence of one or several meniscii introduce capillary forces as a third factor. Consequently such flows provide a rich source of instabilities and pattern formation processes [13–15].

To simplify the geometrical complexity, we observed the progress of a gas/liquid meniscus along a tube filled with sedimented granular mixture of liquid and glass beads [16]. The confinement chosen is approaching a one-dimensional geometry. We are reporting here the response of a confined granular material under capillary bulldozing.

## 2 Materials and Methods

A long horizontal tube of size $L = 1.0$ m with constant diameter $D = 2$ mm is filled with a sedimented mixture of liquid and glass beads, with reduced filling fraction $\varphi = \phi_0/\phi_c$, defined as the ratio between the volume fraction $\phi_0$ of grains in the grain-water mixture, and the random close packing $\phi_c$. Glass beads are sieved to control the polydispersity. The tube is pumped at constant withdrawing rate $I_0$ and the pressure at the tube's outlet is recorded, see Fig. 1 (a). The tube's diameter is chosen to not exceed the capillary length of the liquid used, ensuring that the meniscus fills the tube's aperture, without spreading along the tube, see Fig. 1 (b). The inner surface of the tube were treated with a silanization solution to achieve an hydrophobic coating ensuring a contact angle $\geq 90^o$ between the meniscus and the confining walls. The experiment is imaged against an LED screen. At the early stages of the withdrawing, the meniscus progresses along the tube, perturbs the sedimented granular material, see Fig. 1 (b), and forms a growing accumulation front, see Fig. 1 (c). At slow withdrawing rates the capillary

⋆e-mail: guillaume.dumazer@fys.uio.no

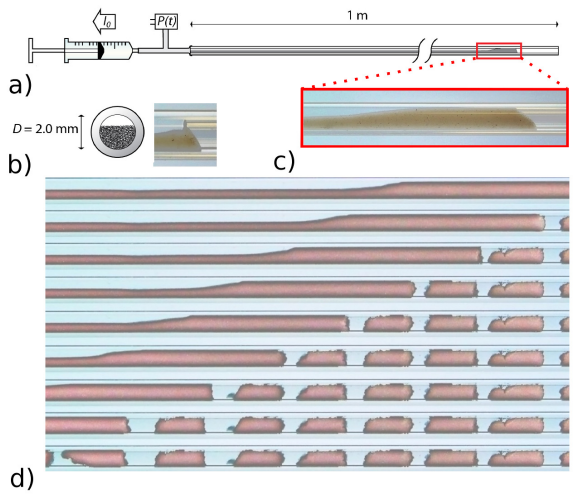


**Figure 1.** (a) Schematic view of the experimental setup. The sedimented glass beads and liquid mixture is withdrawn by a syringe pump at constant withdrawing rate $I_0$, withdrawing pressure is recorded at the tube's outlet. (b) (left) initial cross-section schematics, and (right) zoom over the meniscus just after the withdrawing starts. (c) accumulation front after start of withdrawal. (d) series of pictures showing the accumulation front progress, and the trail of plugs left behind, time develops downwards.

bulldozing leads to the intermittent splitting of the growing accumulation front, and a series of granular plugs are left in the tube, see Fig. 1 (d).

## 3 Plus Formation

The formation of a single plug is imaged after correcting the variations of illumination by subtracting a blank image of the screen, see Fig. 2 (a). Images are then thresholded to clearly distinguish the glass beads from the background. The number of glass beads' pixels are counted as a function of tube's axis $x$. Repeating this operation for every image recorded during the experiment we get a dimensionless signal $s(x,t)$ with 0 value for no glass beads, 1 value for a fully filled tube's cross-section, $s_0$ value for unperturbed sedimented glass beads. By mapping $s(x,t)$ with a colorscale on a spatio-temporal diagram with time developing downwards, and tube's axis horizontally, we get a useful visualization of a single plug formation, see Fig. 2 (b). The formation of a single plug can be decomposed into 4 steps: (i) driven by the syringe pump the meniscus progresses against the sedimented grains which slowly compactifies into a growing accumulation front $(t_1, t_2)$. The frictional interaction between the granular material and the confining wall increases. The Janssen's description of stress in confined granular material [14, 17, 18] suggests here an exponential increase of the pressure with the accumulation front length $P \approx \sigma_0(\varphi, \mu, D) \exp(L/\lambda)$. In this description a slice of compacted granular material is considered. The radial stress $\sigma_{rr}$ normal to the cylindrical confining walls is assumed to be proportional to the longitudinal stress $\sigma_{xx}$, $\sigma_{rr} = K\sigma_{xx}$ with the Janssen's coefficient $K$. The frictional length $\lambda = D/(4\mu K)$ is derived from the force balance over the slice of granular material. (ii) the pressure imposed by the syringe pump reaches the pore pressure of the compacted granular material, $P_{pore} = 4\gamma/d_{pore}$ with the surface tension $\gamma$, allowing the meniscus to bend into interstitial pores of diameter $d_{pore}$. Air quickly percolates through the compacted glass beads and the liquid is pushed away towards the tube's outlet $(t_3, t_4)$. The rapid liquid flow can be considered as a Darcy flow. The viscous forces acting on the compacted grains counteract the frictional interactions, which eventually leads to destabilize the still-immersed packing, and to split the drained glass beads which forms a plug $(t_4)$. (iii) the elastic energy stored in the system during the slow compaction phase is released and the accumulation front rapidly grows $(t_4, t_5)$ before settling down as the next slow compaction phase starts $(t_5, t_6)$. This cycling process is repeated until the meniscus reaches the tube's outlet. The intermittent nature of the plugs formation can be seen from the spatio-temporal diagram obtained over a larger fraction of the tube, see Fig. 3 left for the smallest withdrawing rates.

## 4 Flow Regimes

The formation of plugs corresponds to an instability resulting from the competition between frictional and viscous forces. At low withdrawing rates the granular material settles easily and frictional forces can be established among granular particles as well as with the confining walls. Increasing the withdrawing rate corresponds to increasing the viscous forces in the system. Viscous drag on particles prevent frictional interactions to be established and the granular packing gets fluidized more easily. We observed the various behaviours of the confined glass beads for larger values of withdrawing rates $I_0 \in [0.01, 30]$ mL.min$^{-1}$, and reported in Fig. 3 the corresponding spatio-temporal diagrams obtained. As the withdrawing rate is lower than $\approx 0.3$ mL.min$^{-1}$ the frictional forces are large enough to form the pattern of granular plugs separated by gaps. Larger withdrawing rate, $I_0 \in [0.3, 3]$ mL.min$^{-1}$ weakens frictional interactions. The accumulation front is getting larger as stronger fluidizations occur, and fewer plugs are formed. Another flow regime is obtained for large flow rate $I_0 \leq 3$ mL.min$^{-1}$. The viscous forces dominates and prevent any frictional interactions between grains. Glass beads get suspended and no plugs are left in the tube. These three distinct regimes are denoted respectively the frictional, transitional and viscous flow regimes.

## 5 Phase Diagram

The size of the glass beads influences the balance between friction and visosity. Small glass beads get easily suspended whereas large glass beads are more stable under viscous flow. The viscous drag of a flow through a porous media is indeed proportional to its permeability. A bed

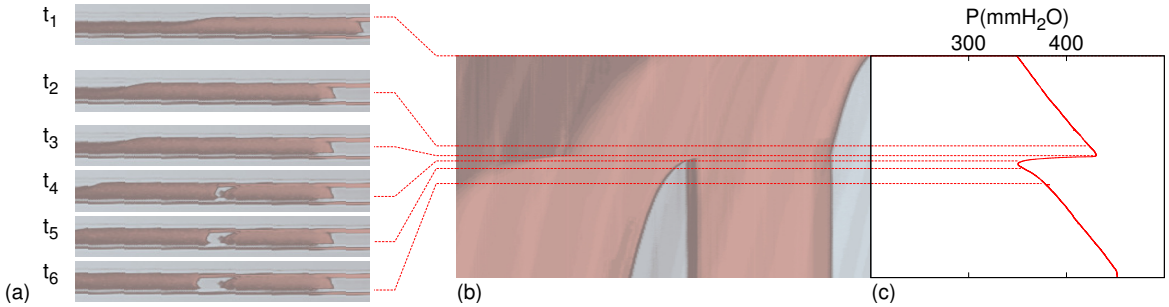


**Figure 2.** Focus over one plug formation obtained for $I_0 = 0.01$ mL.min$^{-1}$, filling fraction $\varphi = 0.5$, beads size $d = [75 - 100]$ $\mu$m illustrated by (a) images and (b) spatio-temporal diagram. (c) pressure measured at the tube's outlet in mmH$_2$O during the plug formation.

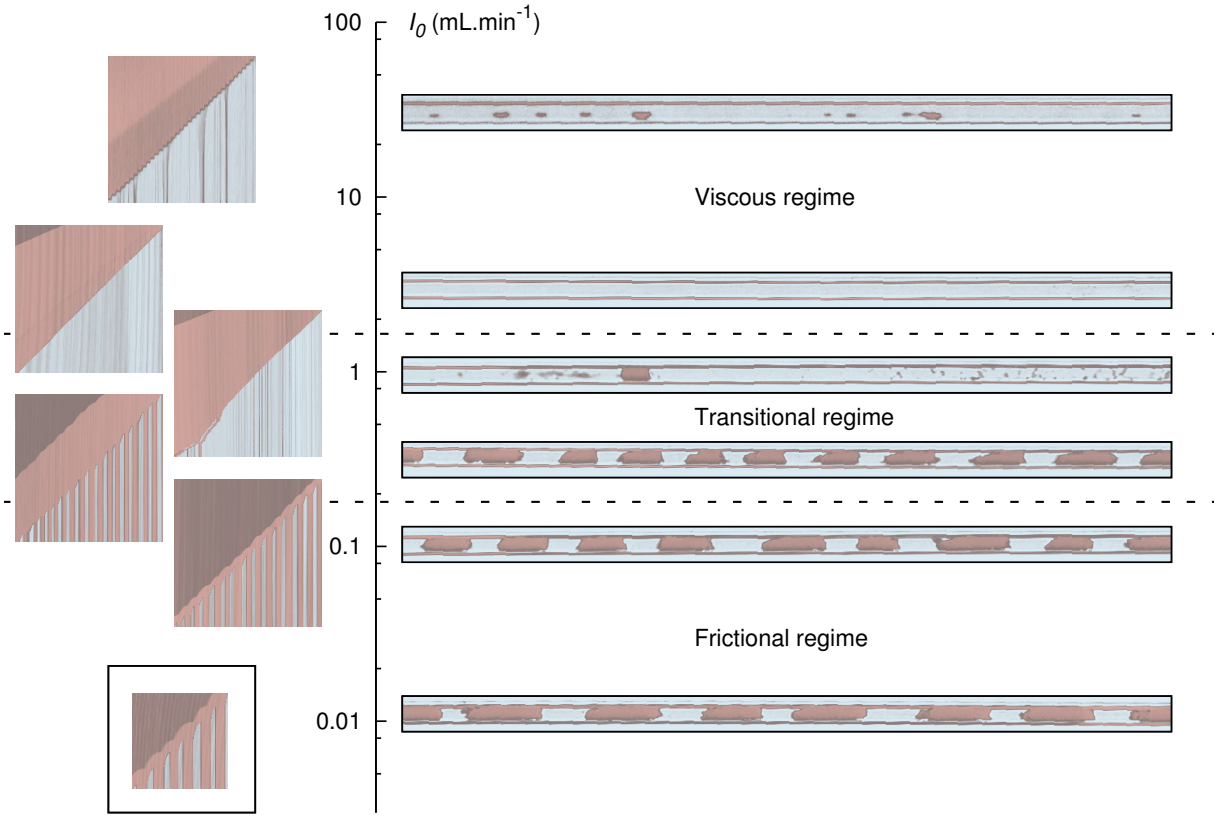


**Figure 3.** (left column) spatio-temoral diagrams obtained with withdrawing rate increase in the range [0.01 – 30] mL.min−1. The reduced units correspond here to a fraction of the total withdrawing time $\tau$ required to empty the tube of size $L$ at withdrawing rate $I_0$. The same filling fraction $\varphi = 0.5$ and beads size $d = [75, 100]$ $\mu$m is used for all observations. Note that at the lowest withdrawing rate $I_0 = 0.01$ mL.min$^{-1}$, the total withdrawing time $\tau$ exeeds the recording time so a smaller fraction of the total spatiotemporal diagram is shown. (right column) corresponding images of the final states obtained. Frictional, transitional and viscous flow regimes are distinguished by the dashed lines according to the qualitative differences in the observations.

of granular particles has a permeability increasing as the particles size decreases, as suggested by the the theoretical Carman-Kozeny relationship. So glass beads were sieved into 5 size ranges [53 – 75], [75 – 100], [100 – 150], [150 – 200], and [200 – 300] $\mu$m. A systematic exploration of the three flow regimes described above has been conducted for every size ranges. Figure 4 gives a phase diagram summarizing the observations with squared beads size horizontally, and imposed flow rate vertically. Observations corresponding to frictional, transitional, or viscous flow regime are pointed respectively with disks, open circles, and solid squares.

## 6 Conclusion

We observed the self structuring of a confined granular material and liquid mixture under capillary stress. A gas/liquid meniscus driven along a narrow tube by a

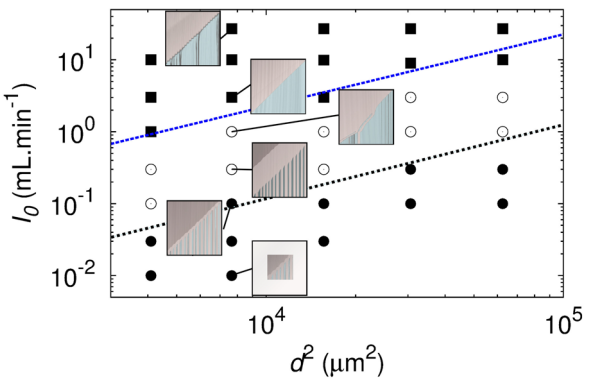


**Figure 4.** Phase diagram featuring the various flow regimes obtained when varying the withdrawing rate $I_0 \in [0.01, 30]$ mL.min$^{-1}$, and the bead sizes $d \in [53-75]$, $[75-100]$, $[100-150]$, $[150-200]$, and $[200-300]$ $\mu$m obtained after sieving. Disks, circles and squares represent respectively frictional, transitional and viscous flow regime. Spatio-temporal diagrams observed in fig 3 are indicated. Dashed lines are used for flow regime demarcations.

syringe pump bulldozes sedimented glass beads and forms regular granular plugs spaced with empty gaps, or suspends and evacuates the granular material from the tube. Three flow regimes are put in evidence as determined by the imposed flow rate as well as the granular particles sizes. The simplified quasi one-dimensional setup presented here provides a useful tool to interprete the complex behaviour of confined granular material in 2D Hele-Shaw cells under capillary stress [13–15].
The complexity of the patterns observed in confined frictional fluid derives from a mixture of capillary, frictional and viscous interactions. Our setup is constraining the frictional fluid by reducing one degree of freedom in comparison to regular Hele-Shaw cells. A subsequent structuring is still occurring as the confinement preserves the internal fluid self-structuring.

## Acknowledgements

This work has been supported by the Norwegian Research Council through the FRINAT Grant No. 213462/F20. B. S. ackowledges support from EPSRC Grant No. EPL/013177/1 and Sêr Cymru National Research Network in Advanced Engineering and Materials Grant No. NRN141.

## References

[1] J. Trondvoll and E. Fjær, Int. J. Rock Mech. Min. Sci. Geomech. Abstr. **31**, 393 (1994)
[2] D. Gidaspow and J. Huang, Ann. Biomed. Eng. **37**, 1534 (2009)
[3] J. B. Freund and M. M. Orescanin, J. Fluid Mech. **671**, 466 (2011)
[4] O. Molerus, Powder Technol. **88**, 309 (1996)
[5] E. Rabinovich and H. Kalman, Powder Technol. **207**, 119 (2011)
[6] M. Strauss, S. McNamara, and H. J. Herrmann, Granular Matter **9**, 35 (2007)
[7] S. Shaul and H. Kalman, Powder Technol. **256**, 310 (2014)
[8] F. B. Soeypan, S. Cremaschi, C. Sarica, H. J. Subramani, and G. E. Kouba, AlChE J. **60**, 76 (2014)
[9] F. Boyer, E. Guazzelli, and O. Pouliquen, Phys. Rev. Lett. **107**, 188301 (2011)
[10] A. Fall, F. Bertrand, G. Ovarlez, and D. Bonn, Phys. Rev. Lett. **103**, 178301 (2009)
[11] R. Seto, R. Mari, J. F. Morris, and M. M. Denn, Phys. Rev. Lett. **111**, 218301 (2011)
[12] E. Brown and H. M. Jaeger, Rep. Prog. Phys. **77**, 046602 (2014)
[13] B. Sandnes, E. G. Flekkøy, H. A. Knudsen, K. J. Måløy, and H. See, Nat. Comm. **2**, 288 (2011)
[14] H. A. Knudsen, B. Sandnes, E. G. Flekkøy, and K. J. Måløy, Phys. Rev. E **77**, 023301 (2008)
[15] C. Chevalier, A. Lindner, M. Leroux, and E. Clément, J. NonNewton. Fluid **158**, 63 (2009)
[16] G. Dumazer, B. Sandnes, M. Ayaz, K. J. Måløy, and E. G. Flekkøy, Phys. Rev. Lett. **117**, 028002 (2016)
[17] H. A. Janssen, Z. Ver. Dtsch. Ing. **39**, 1045 (1895)
[18] B. Marks, B. Sandnes, G. Dumazer, J. A. Eriksen, and K. J. Måløy, Front. Phys. **3**, 41, (2015)